Observations and Simulations of the Stable Water Isotope Signature of Shallow Trade Wind Clouds

Leonie Villiger[1], Marina Dütsch[2], Heini Wernli[1], and Franziska Aemisegger[1]

Contact: leonie.villiger@env.ethz.ch

[1]Institute for Atmospheric and Climate Science, ETH Zurich, Zurich, Switzerland, [2]Institute of Meteorology and Geophysics, University of Vienna, Vienna, Austria

1. Introduction

Shallow trade-wind clouds are a source of uncertainty in climate projections. The coupling between clouds, convection and circulation is still largely a mystery. Here, we present airborne stable water vapour isotope measurements from EUREC⁴A[(1)] and complementary simulations using COSMO$_{iso}$[(2)], which characterise the water vapour at cloud base and possibly point towards different processes depending on the prevailing cloud organisation pattern[(3)].

Q1 Does COSMO$_{iso}$ reproduce the observed isotope signals and cloud organisation patterns?
Q2 Are the archetypal mesoscale cloud organisation patterns in the Trades associated with different isotope signals?
Q3 Is the transport history of importance for the air parcels' isotope signature when arriving in the subtropics?

2. Measurements onboard the ATR-42[(1)]

- 19 flights (each ~4.5h) upstream of Barbados on 11 days between 25 Jan and 13 Feb 2020
- different flight segments with most time spent at cloud base in the so-called *cloud layer* (rectangular flight pattern)

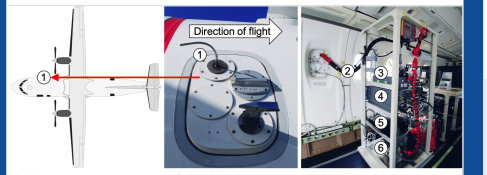

Figure 2.1 Measurement setup during EUREC⁴A with the laser spectrometer Picarro L2130-*i* deployed onboard the French aircraft ATR-42.

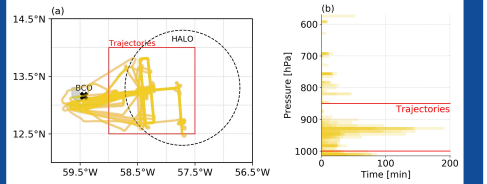

Figure 2.2 Flight path of 19 ATR flights overlayed (yellow). The area from which back-trajectories were calculated (red box/layer). The location of the Barbados Cloud Observatory (BCO) on Barbados and the circle flown by HALO[(0)] shown as black cross and circle, respectively.

3. Simulations with COSMO$_{iso}$

- North Atlantic domain (Fig. 3.1); initial and lateral boundary conditions every 6h from ECHAM6-wiso[(4)] (wind, PS, T nudged to ERA5); horizontal winds at p ≤ 850 hPa nudged to ECHAM6-wiso (wavenumbers ≤ 5)
- hourly output (explicit convection) on 40 vertical levels with 10 x 10 km horizontal resolution from 16 Dec 2019 – 20 Feb 2020
- inside red box (Fig. 2.2): data extraction at three distinct layers (Fig. 3.2) and LAGRANTO[(5,6)] back-trajectories with 20 km horizontal and 15 hPa (1000-850 hPa) vertical spacing

Figure 3.1 Boundaries of the applied COSMO$_{iso}$ domain. The grid is centred at 45°W,25°N and consists of 900 x 800 cells (10 km spacing) on 40 vertical levels. The black cross indicates the BCO and the black circle the circle flown by HALO[(0)]. The 8 day median pathways of the trajectories shown in Fig. 5.2 are illustrated as lines.

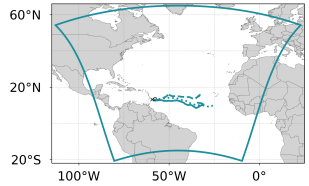

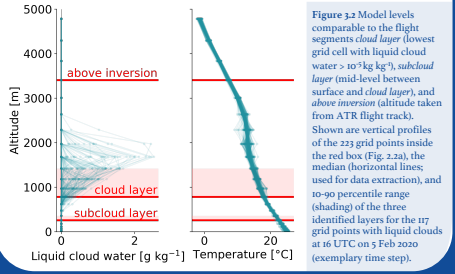

Figure 3.2 Model levels comparable to the flight segments *cloud layer* (lowest grid cell with liquid cloud water > 10^{-5}kg kg^{-1}), *subcloud layer* (mid-level between surface and *cloud layer*), and *above inversion* (altitude taken from ATR flight track). Shown are vertical profiles of the 223 grid points inside the red box (Fig. 2.2a), the median (horizontal lines; used for data extraction), and 10-90 percentile range (shading) of the three identified layers for the 117 grid points with liquid clouds at 16 UTC on 5 Feb 2020 (exemplary time step).

4. Model validation

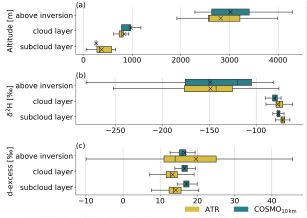

Figure 4.1 Isotope signals in the three layers as boxplots (median as vertical line, mean as cross, 25-75 percentile as box, 10-90 percentile as whiskers, outliers not shown) for COSMO$_{iso}$ data (teal; extracted as described in Fig. 3.2 for the hours with measurements) and ATR data (yellow). The ATR data was averaged over 10 sec after the flight segment assignment.

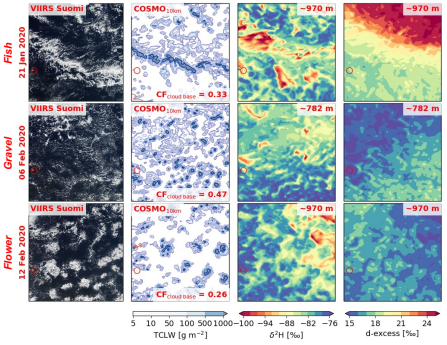

Figure 4.2 Cloud organisation (50-60°W, 10-20°N) shown by (left) Suomi, (centre left) COSMO$_{iso}$ total liquid cloud water and cloud fraction at cloud base (grid cells with liquid cloud water > 10^{-5}kg kg^{-1}), and (centre right/right) δ^2H/d-excess in the *cloud layer* (determined as in Fig. 3.2 using all grid points in the domain) in COSMO$_{iso}$. The dates are not identical to the ones shown in Box 5.

5. Isotopes and cloud organisation

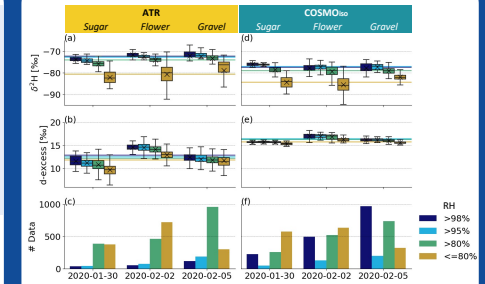

Figure 5.1 Isotope signals in the *cloud layer* during three flights with different cloud organisation patterns (Sugar, Flower, Gravel[(0)] for cloudy (RH>80%) and clear-sky (RH<=80%) environments in the (left) ATR and (right) COSMO$_{iso}$ data. Boxplots as in Fig. 4.1; COSMO$_{iso}$ data extracted as described in Fig. 2.2 for the hours with measurements. (Bottom) data count in seconds for the ATR and in number of grid points during the ATR flight time for the COSMO$_{iso}$ data. The ATR data was averaged over 10 sec after the assignment to the four RH categories.

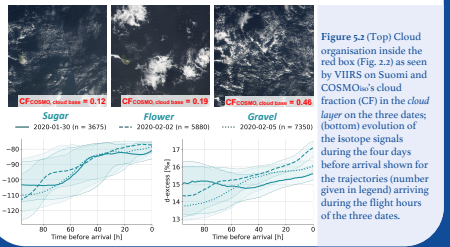

Figure 5.2 (Top) Cloud organisation inside the red box (Fig. 2.2) as seen by VIIRS on Suomi and COSMO$_{iso}$'s cloud fraction (CF) in the *cloud layer* on the three dates; (bottom) evolution of the isotope signals during the four days before arrival shown for the trajectories (number given in legend) arriving during the flight hours of the three dates.

6. Conclusion

C1 COSMO$_{iso}$ underestimates the variability of the observed isotope signals, but qualitatively captures the gradients across different layers (Fig. 4.1). Observed mesoscale cloud organisations are fairly well reproduced in the simulations (Fig. 4.2).
C2 For δ^2H, the in-flight variability is larger than the one between flights. For d-excess it is the other way around (Fig. 5.1) . It is yet unclear how the isotopic signature relates to the mesoscale cloud organisation.
C3 While the δ^2H signal forms shortly (~20 h) before arrival and is most likely controlled by the cloud environment, the d-excess anomaly appears earlier (~50 h before arrival) and is transported towards Barbados (Fig. 5.2).

(1) Stevens, B., et al. (2021), EUREC⁴A. *Earth Syst. Sci. Data*, 10.5194/essd-13-4067-2021
(2) Pfahl, S., et al. (2012). The isotopic composition of precipitation from a winter storm-a case study with the limited-area model COSMOiso. *Atmos. Chem. Phys.*, 10.5194/acp-12-1629-2012
(3) Stevens, B., et al. (2020). Sugar, gravel, fish and flowers: Mesoscale cloud patterns in the trade winds. *Q. J. Roy. Meteor. Soc.*, 10.1002/qj.3662
(4) Werner, M., et al. (2011). Stable water isotopes in the ECHAM5 general circulation model: Toward high-resolution isotope modeling on a global scale. *J. Geophys. Res.-Atmos.*, 10.1029/2011JD015681
(5) Wernli, H., & Davies, H. C. (1997). A Lagrangian-based analysis of extratropical cyclones. I: The method and some applications. *Q. J. Roy. Meteor. Soc.*, 10.1256/smsqj.53810
(6) Sprenger, M., & Wernli, H. (2015). The LAGRANTO Lagrangian analysis tool - Version 2.0. *Geosci. Model Dev.*, 10.5194/gmd-8-2569-2015